Open access • Journal Article • DOI:10.1007/S11104-018-3827-Y

Rhizosphere processes induce changes in dissimilatory iron reduction in a tidal marsh soil: a rhizobox study — Source link

Min Luo, Yuxiu Liu, Jiafang Huang, Leilei Xiao ...+3 more authors

Institutions: Fuzhou University, Fujian Normal University, Chinese Academy of Sciences

Published on: 26 Sep 2018 - Plant and Soil (Springer International Publishing)

Topics: Bulk soil and Rhizosphere

Plant Soil (2018) 433:83–100
https://doi.org/10.1007/s11104-018-3827-y

REGULAR ARTICLE

Rhizosphere processes induce changes in dissimilatory iron reduction in a tidal marsh soil: a rhizobox study

Min Luo · Yuxiu Liu · Jiafang Huang · Leilei Xiao · Wenfeng Zhu · Xun Duan · Chuan Tong

Received: 31 January 2018 / Accepted: 18 September 2018 / Published online: 26 September 2018

Abstract

Background and aims Although the role of microbial iron respiration in tidal marshes has been recognized for decades, the effect of rhizosphere processes on dissimilatory ferric iron reduction (FeR) is poorly known. Herein, we examined the FeR surrounding the root zone of three tidal marsh plants.

Methods Using in situ rhizoboxes, we accurately separated rhizobox soil as one rhizosphere zone, and three bulk soil zones. Dissimilatory and sulfidic-mediated FeR were quantified by accumulation of non-sulfidic Fe(II) and Fe sulfides over time, respectively.

Results The rates of dissimilatory FeR attained 42.5 μmol Fe g^{-1} d^{-1} in the rhizosphere, and logarithmically declined by up to 19.1 μmol Fe g^{-1} d^{-1} in the outer bulk soil. The rates of sulfidic-mediated FeR were less than 2 μmol Fe g^{-1} d^{-1} among all zones. Poorly crystalline Fe(III), DOC and DON, porewater Fe^{2+}, and SO_4^{2-} were all enriched in the rhizosphere, whereas non-sulfidic Fe(II) and Fe sulfides gradually accumulated away from the roots. Iron reducers (*Geobacter*, *Bacillus*, *Shewanella*, and *Clostridium*) had higher populations in the rhizosphere than in the bulk soil. Higher rates of dissimilatory FeR were observed in the *Phragmites australis* and *Spartina alterniflora* rhizoboxes than in the *Cyperus malaccensis* rhizoboxes.

Conclusions The radial change pattern of dissimilatory FeR rates were determined by allocation of poorly crystalline Fe(III) and dissolved organic carbon. The interspecies difference of rhizosphere dissimilatory FeR was associated with the root porosity and aerenchyma of the tidal marsh plants.

Keywords Rhizosphere · Dissimilatory iron reduction · Iron reducers · Root porosity · Tidal marsh

Abbreviations

FeR	Ferric iron reduction
SR	Sulfate reduction
POR	Percentage of root porosity

Responsible Editor: Gustavo Gabriel Striker.

Electronic supplementary material The online version of this article (https://doi.org/10.1007/s11104-018-3827-y) contains supplementary material, which is available to authorized users.

M. Luo · X. Duan
School of Environment and Resource, Fuzhou University, Fuzhou 350116, China

M. Luo
Key Laboratory of Spatial Data Mining & Information Sharing of Ministry Education, Fuzhou University, Fuzhou 350116, China

Y. Liu · J. Huang · W. Zhu · C. Tong (✉)
Key Laboratory of Humid Subtropical Eco-geographical Process, Ministry of Education, School of Geographical Sciences, Fujian Normal University, Shangsan Street #8, Fuzhou City 350007 Fujian Province, China
e-mail: tongch@fjnu.edu.cn

L. Xiao
Key Laboratory of Coastal Biology and Biological Resources Utilization, Yantai Institute of Coastal Zone Research, Chinese Academy of Sciences, Yantai 264003, China

Introduction

The roots of tidal marsh plants are key functional components of belowground systems, and the main agents of coastal soil formation (Mitsch and Gosselink 2015). Rhizosphere processes act mostly via roots releasing oxygen (O_2) and labile C into the soil around the root surface (Bell et al. 2014; Kirwan and Mudd 2012). Even a minor variation in the rhizosphere of marsh plants, could lead to ecosystem-level shifts of whole tidal marshes, and further affect the global carbon (C) cycle (Hinsinger et al. 2009; Lambers et al. 2009).

Iron is the most abundant redox-sensitive metal on Earth (Colombo et al. 2014; Weber et al. 2006). Owing to the presence of roots, the rhizosphere is considered to be a 'hot spot' for Fe biogeochemical cycling (Lemanceau et al. 2009). One of the most well-known processes is Fe plaque precipitation, caused by the oxidization of ferrous iron (Fe(II)) in the rhizosphere, through radial oxygen loss (ROL) from marsh plant roots (Armstrong et al. 2000). The rusty Fe plaque consists of abundant bioavailable ferric iron (Fe(III)) minerals (Colmer and Pedersen 2008). Rhizospheric Fe plaque precipitation has been widely studied in the fields of Fe(II)-oxidizing bacteria (Emerson et al. 2010; Neubauer et al. 2007; Wang et al. 2011; Weiss et al. 2007), the pool and mineralogy of Fe plaque (Crowder and Macfie 1986; St-Cyr and Crowder 1989; Yang et al. 2014), and the potential for Fe(II) oxidation (Laanbroek 1990; Weiss et al. 2004, 2005; Whitmire and Hamilton 2008). However, the rhizosphere could also be an optimal area for Fe(III) reduction (FeR) (Neubauer et al. 2008), as: i) Fe plaque could act as the electron acceptors and electron sink for FeR (Li et al. 2013); ii) root exudates contain abundant dissolved organic matter, which can serve as an effective carbon source (Gribsholt and Kristensen 2002; Hines et al. 1989; Howarth 1993); and iii) rhizosphere processes could offer suitable redox condition for FeR (Hartmann et al. 2009).

There are two basic pathways for FeR in tidal marsh soil: microbial and chemical FeR (Lovley and Phillips 1986). In microbial FeR, iron reducers degrade organic substrates into small-molecular organic acid through fermentation, or into carbon dioxide (CO_2) through respiration (Li et al. 2011). According to previous studies, dissimilatory (microbial respiratory) FeR, contributes to 21–86% of the total organic matter mineralization in many non-sulfidogenic tidal marsh soils (Hyun et al. 2009; Kostka et al. 2002; Luo et al. 2014; Neubauer et al. 2005). In chemical FeR, Fe(III) can be dissolved and reduced by organic acid in the root zone, or can be reduced by free sulfides (H_2S) and produces Fe sulfide minerals, such as FeS (mackinawite) and FeS_2 (pyrite) (Beck et al. 2008; Howarth and Jørgensen 1984; Moeslundi et al. 1994). Sulfide-mediated FeR is also suggested in some research to be abiotic FeR (Hyun et al. 2009; Hyun et al. 2007; Roden and Wetzel 2002). However, this process is not a completely abiotic process, as most of the H_2S is produced by dissimilatory sulfate reduction (SR), which is another dominant organic carbon mineralization pathway in tidal marsh soil (Hyun et al. 2009; Hyun et al. 2007; Kostka et al. 2002). Both dissimilatory and sulfide-mediated FeR have been associated with the organic matter mineralization and carbon cycling in the tidal marsh system.

Recently, we investigated dissimilatory FeR using in situ vegetated and unvegetated mesocosms (Luo et al. 2017). Our results indicated that the presence of plants increases the amount of Fe(III) and organic substrates, and further increases the competitiveness of dissimilatory FeR over SR. Likewise, within vegetated marshes, the availability of oxygen (Armstrong et al. 2000), pH and redox condition (Koop-Jakobsen et al. 2017; Koop-Jakobsen and Wenzhöfer 2015), root exudation (Finzi et al. 2015; Hafner et al. 2014), and enzymatic activity (Ma et al. 2018) have been proven to greatly change within several millimeters in the root zones. These findings suggested that rhizosphere-associated physical and chemical processes, may also stimulate geometry and heterogeneity of FeR within a much smaller scale than previously thought.

With this in mind, we examined the FeR in in situ rhizoboxes, colonized by three different tidal marsh plants of southeast China: two perennial Gramineae plants (*Phragmites australis* (Cav.) Trin. ex Steud. and *Spartina alterniflora* Lois.), and one perennial Cyperaceae plant (*Cyperus malaccensis* Lam. var. *brevifolius* Bocklr.). The present study specifically aimed to: i) investigate Fe speciation, population of typical iron reducers, and the rates and pathway for FeR across the radial profiles surrounding the root zone; and ii) determine the differences in FeR among three tidal marsh plants.

Materials and methods

Soil preparation

Soil samples used in this experiment were collected from the upper 20 cm of a unvegetated creek bank in the Shanyu Tidal Marsh (26°2′0″ N, 119°37′0″ E), in the Min River estuary in southeast China (Fig. 1a, b), which has a typical subtropical monsoon climate (mean annual precipitation = 1785 mm; mean annual temperature = 17.8 °C). The study site is flooded twice daily, and time inundated per month ranged from 26 to 31% according to our previous investigation (Luo et al. 2017). Crabs (*Chiromantes dehaani*) prevail at the study site. Other characteristics of the study site have been described in detail previously (Luo et al. 2017). On March 10, 2016, after carefully removing all visible macrobenthos, the soil was fully pooled, mixed, homogenized, and subsequently passed through a 2 mm sieve for future plant cultivation. The particle size composition of the soil is described as follows: clay 10.3–13.4%, silt 54.3–58.7%, and sand 28.4–35.2%. The soil is characterized as silt loam according to the U.S. Department of Agriculture (USDA) soil classification system. The chemical properties of the soil were: total organic carbon (TOC) 1.12 ± 0.11%, in situ conductivity 2.97 ± 0.25 mS cm^{-1}, in situ pH 7.1 ± 0.2, and in situ salinity 0.25 ± 0.04%. The test method for the above soil properties is described below.

Rhizobox design

The cuboid acrylic rhizoboxes (length = 25 cm; width = 15 cm; height = 15 cm) used in this study, contained three separate top-open compartments that could be screwed together into one assembly (Fig. 1c). The middle compartment was allowed to interact with the surroundings through perforated boards in the bottom and sides. When the plants grow, the roots can gradually fill the rhizoboxes and squeeze some soil out of the middle compartment through the side holes. The perforated partitions together with the double nylon filter cloth (100 mesh, Taizhou Haotian Industrial Fabric Co., Zhejiang Province, China), was placed between the middle compartment and the side compartments. This was designed to allow nutrition and water exchange but prevent the plant roots from penetrating. The outer boards of the side compartments can be removed for soil sampling. The rhizobox system enables soil sampling at defined distances from root compartment (Wang et al. 2018).

In situ plant cultivation and harvest

On March 10, 2016, nine rhizoboxes were arranged 30–50 cm apart in one transect, on the barrier island of east Shanyu Tidal Marsh (Fig. 1b). Here, three dominant marsh plant species, *S. alterniflora*, *P. australis*, and *C. malaccensis* can be found. The natural presence of these species indicated that the soil and hydrology conditions at the study site are suitable for their growth. Soil samples were loaded into all three compartments of the rhizoboxes. Six seedlings of each marsh plant were evenly planted within the root (center) compartments (height: 5–10 cm), one week after the soil transfer. No plants were added to the side compartments. Pieces of 100 mesh nylon filter cloth, and nylon-wire fencing were placed on top of the side compartments to impede macrobenthos incursions. Twenty days after cultivating, one seedling of *P. australis* had died, and was replaced with a nearby naturally occurring seedling, of a similar size and growth stage. On July 18, 2016 (ambient temperature 32 °C), all marsh plants in the rhizoboxes had grown vigorously, and the rhizoboxes were full of roots. During the ebb tide, all rhizoboxes were taken out of the ground and wrapped in opaque plastic cloth. The chambers were stored on ice and taken back to the laboratory within an hour.

Sample collection and preparation

In the laboratory, pretreatment of the soil and porewater samples was conducted in a nitrogen (N_2) filled glove bag (AtmosBag, Sigma-Aldrich, USA). The potential air-oxidized surface layer of the soil (approximately 0–2 cm) was removed, in order to focus on the rhizosphere processes. After pulling up the removable outboards, sub-samples of each interval were stepwise extruded outward. Soil inside the side compartments was sliced at 2 mm, 5 mm, 10 mm, 15 mm, 20 mm, 25 mm, 50 mm, and 100 mm away from the root compartments using several sharp stainless sheets. Soil inside the root compartments was carefully removed roots and other plant residues. Before further preservation, soil-subsamples from each interval were pooled and homogenized, and sieved <2 mm. Porewater was extracted via in situ Rhizon samplers in the closed plastic bags under an N_2 atmosphere (Seeberg-Elverfeldt et al. 2005). All

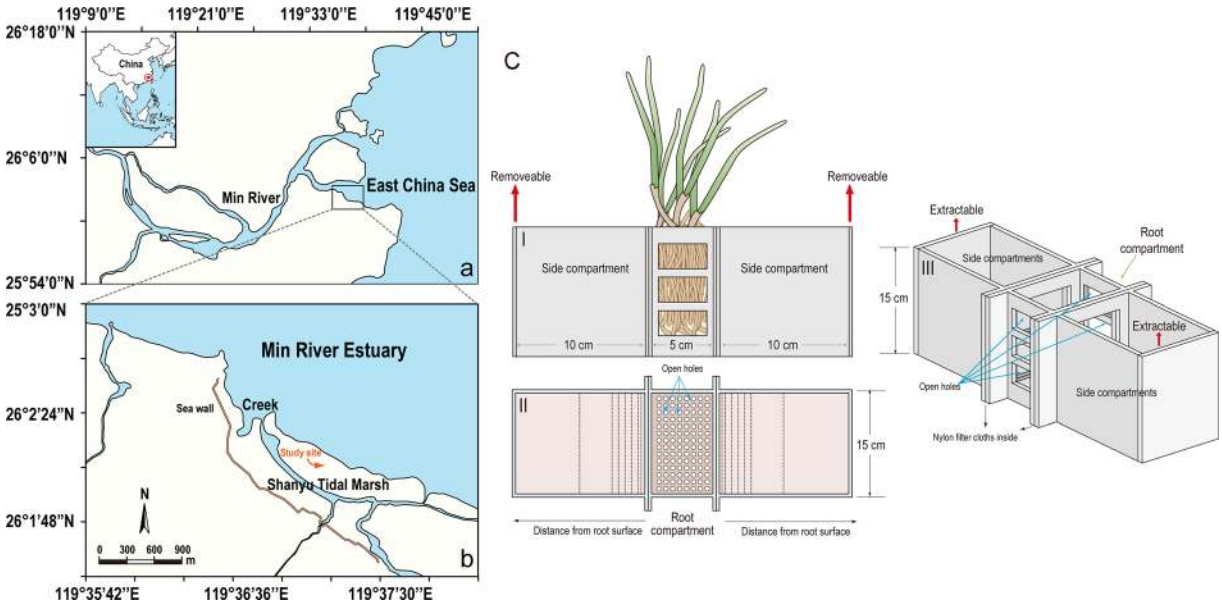

Fig. 1 Location of the rhizoboxes in the (**b**) Shanyu Tidal marsh, of (**a**) the Min River estuary in the East China Sea, and (**c**) diagram showing the design of the rhizoboxes (i) side view, (ii) top view, and (iii) three-dimensional view), and the radial sampling strategy

porewater samples were filtered through 0.45 μm syringe filters with a GH Polypro membrane (Acrodisc, Pall Corporation, New York, USA; Karanfil et al. 2003), and drained into 5 mL glass vials. For filter effectiveness of each index, we used a standard solution to test our wash process and leaching potentials. Filters used for Fe^{2+} and DOC analyses were preserved with diluted HCl solution; NO_3^- and NH_4^+ analyses were preserved by 0.1 M mercuric chloride; and SO_4^{2-} analyses were preserved by 0.2 M deoxygenated nitric acid. Porewater samples were then stored in bottles capped with Teflon-coated butyl rubber septa. Samples for chemical property analysis were stored at 4 °C; whilst other samples were snap frozen in liquid nitrogen and stored at −80 °C for DNA extraction. For further analysis, we operationally defined the middle root compartment as the rhizosphere, soil from 0 to 5 mm intervals in the side compartment as the inner bulk soil zone, 5–15 mm intervals in the side compartment as the middle bulk soil zone, and 15–100 mm intervals in the side compartment as the outer bulk soil zone (Li et al. 2008; Wang et al. 2018).

Plant trait analysis

Three healthy adventitious roots were collected from each rhizobox. Fresh root samples (approximate root diameter 0.8–1.2 mm, root length 5–9 cm), of three marsh plants were selected, and sections (approximate 5 mm from the root tips), were prepared according to previous studies (Li et al. 2008; Longstreth and Borkhsenious 2000). The root samples were viewed and photographed on a field emission scanning electron microscope (JSM-7200F; JEOL; Tokyo; Japan).

The amount of aerenchyma was also measured by the percentage of root porosity (POR, %), a method developed by Kludze et al. (1993). Briefly, about 0.4 to 0.6 g of fresh and healthy roots were selected from the adventitious roots and dried on filter paper. Root samples were cut 2 to 2.5 cm from the root apex and then loaded into 25 mL pycnometers, which had been filled with deionized water and weighed before the root addition, and then reweighed and subjected to vacuum in the pycnometers for 2 h. The roots were later retrieved, ground into a paste with a mortar and pestle, and returned to the pycnometer for reweighing. POR was determined by Eq. 1 (Li et al. 2008):

$$\mathrm{POR} = \left[\left(P_{gr}–P_r\right)/\left(r + P–P_r\right)\right] \quad (1)$$

where P_{gr} is the mass of the pycnometer with water and ground roots (g), P_r is the mass of the pycnometer with water and roots (g), r is the mass of roots (g), and P is the mass of the pycnometer with water (g).

The aboveground and belowground biomass (including all living and dead roots and shoots) were heated at 105 °C. Then, the samples were oven-dried at 70 °C for

48 h until their biomass was constant. The fresh root mass used for SEM and POR testing, were corrected for in the final belowground biomass weight.

Soil and porewater geochemistry

Total organic carbon (TOC) was analyzed by a CHNS analyzer (Vario EL III, Elementar, Hanau, Germany). Before determination, inorganic carbon was removed with 10% HCl. The in situ conductivity, pH, and salinity were detected with an Eutech sensor (Testr11+, Thermo Fisher Scientific Inc., MA, USA), a pH 400 m (Spectrum, WI, USA), and an Eutech salinity meter (Salt6+). Particle size was determined via Mastersizer 2000 laser diffraction (Malvern Instruments, UK).

The solid Fe species (all given on a dry mass basis), were extracted by the procedure developed by Kostka and Luther III (1994). Briefly, the HCl-extractable Fe(II) was determined by extraction, using 0.5 M deoxygenated HCl for 1.5 h (APHA 2005). The total HCl-extractable Fe concentrations were determined via dissolution with 0.5 M deoxygenated HCl plus 0.1 $g{\cdot}mL^{-1}$ hydroxylamine (APHA 2005). The concentration of HCl-extractable Fe(III) (i.e., poorly crystalline Fe(III)) equals the difference between total HCl-extractable Fe and HCl-extractable Fe(II). After HCl extraction, the crystalline Fe(III) was determined by subsequent extraction, using citrate-bicarbonate-dithionite (CBD; 0.35 M glacial acetic acid/0.2 M sodium citrate, buffering with 50 $g{\cdot}L^{-1}$ of sodium dithionite), on the residual soil. All above Fe species were examined using 1,10-phenanthroline colorimetric method (APHA 2005) via UV spectrophotometry (2450, Shimadzu, Kyoto, Japan). The recovery of Fe(II), poorly crystalline Fe(III), and crystalline Fe(III) were assessed in triplicate by $FeCO_3$ (AR, >98.0% purity), ferrihydrite (synthetic, >99.0% purity, Poulton and Canfield 2005), and α-FeOOH (synthetic, >98% purity, Poulton and Canfield 2005), and was found to be 95–101%, 96–100%, and 92–102%, respectively.

Solid-phase analyses for sulfur species (including acid-volatile sulfide (AVS) and chromium-reducible sulfide (CRS)) was performed by the procedure and apparatus developed by Burton et al. (2008). Briefly, the AVS concentration was determined by extracting using 0.1 M ascorbic acid solution / 6 M HCl, adsorbed by zinc acetate solution. The CRS concentration was determined from the residual via acid $CrCl_2$ solution, adsorbed by zinc acetate solution. All above S species were examined using Methylene blue colorimetric method (Cline 1969) via UV spectrophotometry (2450, Shimadzu, Kyoto, Japan). The recovery of reduced AVS species were assessed in triplicate by Na_2S (AR, >98.0% purity), and pyrite (>98% purity, obtained from the Yunfu Guangye Pyrite Group Limited, China), and it was found to be 94–98% and 96–100%.

Porewater analyses for ferrous iron (Fe^{2+}) were examined using 1,10-phenanthroline colorimetric assay (detection limit = 1 μM; SD = 1%). Dissolved organic carbon (DOC) was examined via TOC analyzer (TOC-V CPH, Shimadzu, Kyoto, Japan; detection limit = 2 μM; SD = 5%). Porewater SO_4^{2-} was examined by Ion chromatograph (ICS2100, Dionex Corporation, CA, USA; detection limit = 3 μM, SD = 6%). The estimates of ferrous sulfide (FeS), and pyrite (FeS_2), were based on the stoichiometric relationship between Fe and S in AVS (Fe:S = 1:1 in AVS), and CRS (Fe:S = 1:2 in CRS). The non-sulfidic Fe(II) concentration was calculated based on the difference between Fe(II) and iron sulfides (non-sulfidic Fe(II) = Fe(II) − FeS) (Johnston et al. 2011). To test whether 0.5 M HCl could extract FeS, the recovery test was given in the supplementary material (Table S1).

Mineralogy

The soil samples for investigating mineralogy of iron oxyhydroxides were prepared according to previous studies (Luo et al. 2014; Schulze 1981). The mineralogy of the soil was detected through an X-ray diffraction system (X'pert3, Empyrean, Panalytical, Netherlands). Mineralogical analysis was performed using Jade 6.0 software (MDI, CA, USA).

Rate measurements

Incubation experiments were also conducted, as described in detail by Luo et al. (2017). Briefly, each sub-sample (containing approximate 5 g wet soil) was loaded into a 7 mL glass vial. The jars were capped tightly with Teflon-coated butyl rubber septa and stored in the dark at the field temperature (32 °C) for 48 h. At regular intervals (24 h), three vials were used for rate measurements of dissimilatory FeR and another three were used for sulfide-mediated rates. The dissimilatory FeR rates were estimated from the production of non-sulfidic Fe(II) and porewater Fe^{2+} over time, whilst the production of FeS and FeS_2 over time was used to

determine the sulfide-mediated FeR rate (Kostka et al. 2002; Hyun et al. 2009). The rates of dissimilatory FeR ($r^2 > 0.94$), and sulfide-mediated FeR ($r^2 > 0.87$), were typically linear over the 48 h incubation period**.** Note that as our incubation experiments were under a strict anaerobic condition with root-free soil, any measured rhizosphere effects on soil processes should be considered as occurring before the incubation began.

Microbial analyses

Soil DNA was extracted using a FastDNA SPIN Kit (BIO101, Vista, CA, USA). Bacterial abundance, indicated by the 16S rRNA gene copy number, was quantified by real-time PCR (qPCR). The lack of a universal functional gene marker made it difficult to track all iron reducers, especially those of rare taxa (Peng et al. 2016). Based on previous investigations of 16S rRNA gene sequences in the Shanyu Tidal Marsh of the Min River estuary (data not published), *Geobacter*, *Shewanella*, *Anaeromyxobacter*, *Bacillus*, and *Clostridium* sensu stricto 12 were identified in the tidal marsh soil. Thus, we selected these five specific Fe(III)-reducer species. However, we acknowledged that some important genera would still be missed.

Bacteria domain-specific (com1, com2) (Muyzer et al. 1995), and specific primers for *Geobacter* (GM3, 825R) (Holmes et al. 2002), *Bacillus* (B-K1, B-K1) (Wu et al. 2006b), *Shewanella* (Shw783F, Shw1245R) (Snoeyenbos-West et al. 2000), *Anaeromyxobacter* (Ab112F, Ab227R) (Wu et al. 2006a), and *Clostridium* (Chis150F, ClostIR) (Hung et al. 2008), were used. Note that a general probe used for *Clostridium* and *Bacillus* may result in an overestimation for iron reducers. The qPCR was performed on an iQ™5 thermocycler (Bio-Rad, Hercules, CA, USA). The PCR mixtures were incubated first at 94 °C for 60 s, followed by 40 cycles of denaturing at 94 °C for 30 s, annealing at 60 °C for 30 s, extending at 72 °C for 30 s, and extending once again at 72 °C for 2 min.

Data analysis

All data sets were tested to meet the assumptions of homogeneity and normality. If these assumptions were not met, the data was log transformed before further analysis. Two-way ANOVAs were utilized to make comparisons among the rhizobox zonation among the three different plants. In some cases, the ANOVA was followed by the Tukey post hoc test to determine if the radial rhizobox zones or plants differed significantly. Non-parametric tests (K sample) were used to make comparisons of microbes between the rhizosphere and bulk soil, and among plant species. Paired sample *t*-tests were used to compare the rates of dissimilatory FeR with sulfide-mediated FeR, and concentrations of FeS with FeS_2. Pearson's correlation was used to analyze the relationships between rates of dissimilatory FeR and chemical properties, and plant straits. Nonlinear regression was used between the rates of dissimilatory FeR and the distance from the root zones. For all analyses, a significance level of $\alpha = 0.05$ was used. Differences in the ANOVA, regression, and correlation analyses were considered to be statistically significant when $p < 0.05$. Data were provided as mean ± standard error (SE) unless indicated otherwise. Statistics 22.0 software was used to perform all statistical analyses.

Results

Plant traits

After 130 days of in situ cultivation, living and healthy marsh plant roots filled the rhizoboxes, with abundant Fe plaque coating present on the root surfaces (Figs. 2a, b and c). The aboveground biomass (kg m^{-2}) of *S. alterniflora* was significantly higher than that of *P. australis* and *C. malaccensis*, while the belowground biomass (g cm^{-3}) was similar among the three plant species **(**Table 1**).** Porosity of root (POR, %) of *C. malaccensis* was found to be significantly lower compared to the other two marsh plants (Table 1). SEM photographs showed that most of the cortical parenchyma cells of all three plants had collapsed and dissociated, forming apparent air flow chambers (Figs. 2d, e and f). *Spartina alterniflora* and *P. australis* developed root aerenchyma that looked like wheel spokes, while *C. malaccensis* developed root aerenchyma that looked like radial spider webs (Figs. 2d, e and f). Some parenchyma cells of *C. malaccensis* had not totally collapsed, and residual cells could be observed between the stele and epidermis layers (Fig. 2f). The cells were arranged more closely in *C. malaccensis* compared with

those in *P. australis* and *S. alterniflora* (Figs. 2d, e and f), suggesting better-developed aerenchyma in *P. australis* and *S. alterniflora* compared with *C. malaccensis*, which is also consistent with the POR results (Table 1). Significant correlation was also observed between POR and rhizospheric poorly crystalline Fe(III) concentrations (Fig. S2a), and Fe(III):Fe(II) ratios of three tidal marsh plants (Fig. S2b).

Soil and porewater geochemistry

The concentrations of DOC and DON (Fig. 3a, b, mg C L^{-1} and mg N L^{-1}, respectively), ranged from 7.4 to 72.0, and from 0.6 to 4.1, respectively. The concentrations of DOC and DON changed significantly among the radial zones (Table 2), following the order: rhizosphere > inner bulk soil > middle and outer bulk soil (Table 3). The concentrations of DOC and DON were higher in the *S. alterniflora*, followed by *C. malaccensis* rhizoboxes, compared to those in the *P. australis* rhizoboxes (Table 4).

Porewater SO_4^{2-} (Fig. 3c, mM) smoothly declined in the radial direction with the maximum in the rhizosphere (mean of 6.5), followed by inner bulk soil (mean of 6.0), and then middle and outer bulk soil (mean of 4.6 and 3.8, respectively) (Table 3). The concentrations of porewater SO_4^{2-} were comparable among the three marsh plants (Table 2).

For the porewater Fe^{2+} (Fig. 3d; μM), concentrations were highest in the rhizosphere (mean: 682), and lowest in the outer bulk soil (mean: 159), of all rhizobox zones. The interaction of radial zonation and plant species also had a significant influence on Fe^{2+} concentrations (Table 2). *Cyperus malaccensis* had lower Fe^{2+} concentrations in the rhizosphere and inner rhizosphere zone than *P. australis* and *S. alterniflora*, but comparable values in the middle and outer bulk soil (see supplementary material Fig. S1a).

The concentrations of all solid-phase Fe species (μmol Fe g^{-1} based on dry weight) are given in Fig. 4. Poorly crystalline Fe(III) concentrations significantly decreased from the rhizosphere (mean: 95.2) to the outer bulk soil (mean: 34.2; declining to ~36%) (Table 3). For crystalline Fe(III), concentrations were higher in the rhizosphere (mean: 64.0) compared with the three bulk soil zone (range: 52.6–57.3) (Table 3). Non-sulfidic Fe(II) increased ~2.4 times from the rhizosphere (mean: 21.8) to the outer bulk soil (mean: 52.1) (Table 3). The ratios of Fe(III):Fe(II) were 5.1 in the rhizosphere, declining to 2.8 in the inner bulk soil, and then 0.9 to 1.5 in the outer and middle bulk soil, respectively (Table 3). Fe sulfide concentrations ranged from the lowest in the rhizosphere (mean: FeS = 1.5; FeS_2 = 9.3) to the highest in the outer bulk soil (mean: FeS = 18.2, about 12.1 times greater; FeS_2 = 20.8, about 2.2 times greater) (Table 3). The concentrations of FeS_2 were significantly higher than that of FeS in all rhizoboxes (df = 80, T = 8.358, $p < 0.001$). The soil in *S. alterniflora* and *P. australis* rhizoboxes had higher Fe(III):Fe(II) ratios and poorly crystalline Fe(III) concentrations compared to *C. malaccensis* rhizoboxes (Table 4). Moreover, the interaction of radial zonation and plant species also had a significant influence on poorly crystalline Fe(III) concentrations (Table 2). *Spartina alterniflora* had significantly lower poorly crystalline Fe(III) concentrations in the rhizosphere than *P. australis* and *C. malaccensis*. However, *S. alterniflora* had higher or comparable poorly crystalline Fe(III) concentrations than *P. australis* and *C. malaccensis* in the three bulk soil zones (see supplementary material Fig. S1b).

Fe(III) mineralogy

The X-ray diffraction results of the rhizosphere soil demonstrated the presence of poorly crystalline Fe(III) including ferrihydrite, feroxyhyte, lepidocrocite, and crystalline Fe(III) minerals including akaganéite and goethite (Fig. 5). The mineral composition did not apparently change among the rhizosphere of three tidal marsh plants.

Rates of Fe(III) reduction

Rates of dissimilatory FeR and sulfide-mediated FeR (μmol Fe g^{-1} d^{-1}) gradually decreased from the rhizosphere to the bulk soil (Fig. 6). Rates of dissimilatory FeR were comparable among the rhizosphere (mean: 42.5) and inner bulk soil (mean: 38.9), declining to the middle (mean: 34.0) and outer bulk soil (mean: 19.1) (Table 3). Rates of sulfide-mediated FeR gradually decreased from the rhizosphere (mean: 1.7) and the inner bulk soil (mean: 1.5), to the middle (mean: 1.1) and the outer bulk soil (mean: 1.0) (Table 3). Rates of

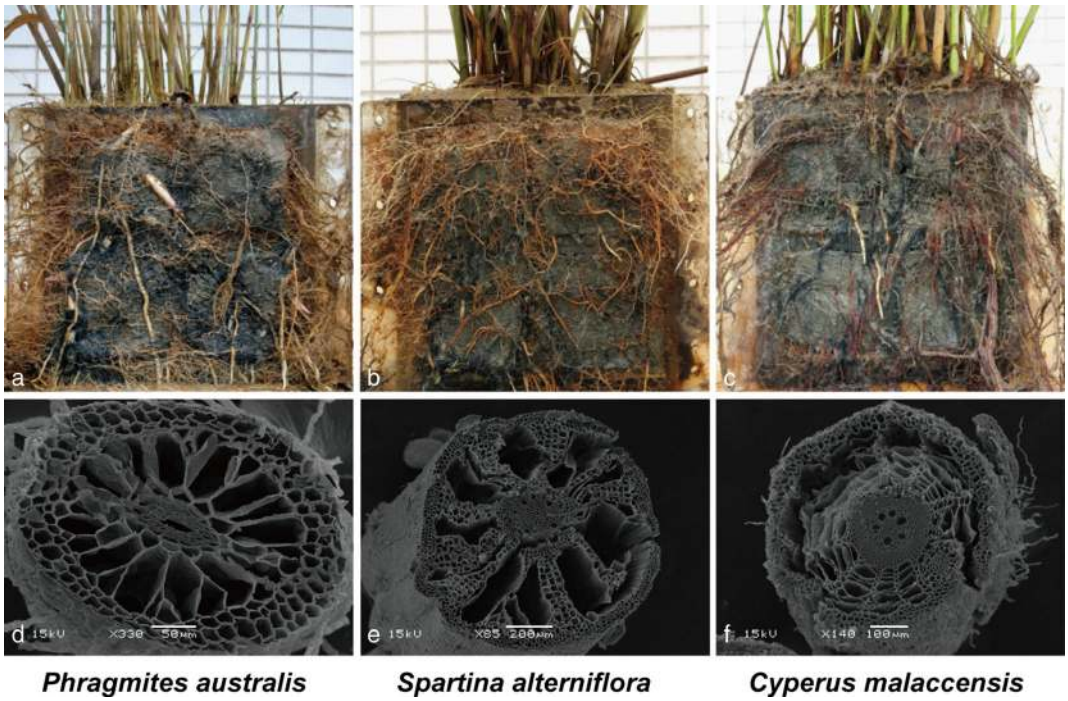

Fig. 2 Cross-profiles of root chambers of marsh plant rhizoboxes, and cross-sectional scanning electron micrographs of the root base (5 mm from the root tip, approximate root diameter 0.8–1.2 mm, root length 5–9 cm) in three marsh plants (d) *Phragmites australis*, (e) *Spartina alterniflora*, and (f) *Cyperus malaccensis*

dissimilatory FeR (μmol Fe g^{-1} d^{-1}) dominated (84–99%) of the sum of dissimilatory and sulfide-mediated FeR in all rhizoboxes. A positive linear relationship was observed between the rates of dissimilatory FeR and concentrations of poorly crystalline Fe(III) and DOC, as well as Fe(III):Fe(II) ratios (Figs. 7a, b and c). Significantly different dissimilatory FeR rates were found among plant species, with the rates lower in *C. malaccensis* rhizoboxes, compared with those in the *S. alterniflora* and *P. australis* rhizoboxes (Table 4). No significant differences in the rates of sulfide-mediated FeR could be observed among the three types of plants (Table 2).

Iron reducers

Populations of total bacteria, total iron reducers, *Geobacter*, *Bacillus*, *Shewanella* and *Clostridium* were higher in the rhizosphere than in the bulk soil among the three marsh plants (Chi > 12.789; $p < 0.05$). *Geobacter*

Table 1 Plant traits (±SE; $n = 3$) from rhizoboxes of *Phragmites australis*, *Spartina alterniflora*, and *Cyperus malaccensis* at the study site in the Min River estuary of the East China Sea, in July 2016

Plant traits	F	Tidal marsh plants		
		P. australis	*S.alterniflora*	*C. malaccensis*
Family		*Gramineae*	*Gramineae*	*Cyperaceae*
CO_2 fixation mode		C3	C4	C4
Aboveground biomass (kg m^{-2}) *	9.295	1.22 ± 0.07 [b]	1.99 ± 0.17 [a]	1.21 ± 0.18 [b]
Belowground biomass (mg cm^{-3}) †	3.060	10.56 ± 0.28 [a]	13.77 ± 0.45 [a]	11.98 ± 1.50 [a]
Porosity of root (%) *	7.821	33.6 ± 0.7 [a]	34.3 ± 1.4 [a]	28.3 ± 1.2 [b]

* The parameters were significantly different among the sites $p < 0.05$; while †denotes that the parameters were insignificantly different among the sites $p > 0.05$

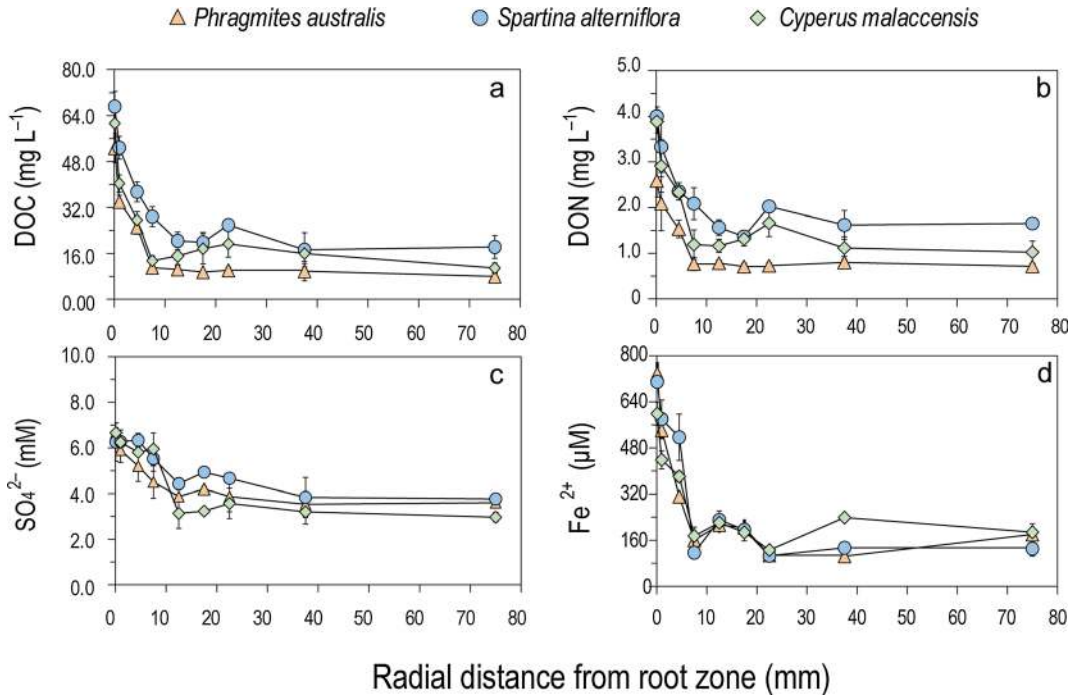

Fig. 3 Radial profiles (n = 3; error bars indicate ± SE) of porewater geochemistry surrounding the root zones in rhizoboxes containing *Phragmites australis*, *Spartina alterniflora*, and *Cyperus malaccensis* in the Min River estuary of the East China Sea in 2016: (**a**) DOC, (**b**) DON, (**c**) SO_4^{2-}, and (**d**) Fe^{2+}

Table 2 Two-way ANOVA analysis of soil and porewater geochemistry, and Fe(III) reduction (FeR) rates from different zones of *Phragmites australis*, *Spartina alterniflora*, and *Cyperus malaccensis* rhizoboxes, at the study site in the Min River estuary of the East China Sea in July 2016

	Rhizobox zone (df = 3)		Plant (df = **2**)		Rhizobox zone × Plant (df = 6)	
	F	P	F	P	F	P
Porewater geochemistry						
DOC (mg L^{-1})	277.326	< **0.001**	46.191	< **0.001**	1.086	0.380
DON (mg L^{-1})	86.819	< **0.001**	22.614	< **0.001**	1.730	0.127
SO_4^{2-} (mM)	70.793	< **0.001**	2.450	0.094	2.044	0.071
Fe^{2+} (μM)	249.305	< **0.001**	3.058	0.053	5.033	< **0.001**
Soil geochemistry						
Poorly crystalline Fe(III)	103.151	< **0.001**	6.179	**0.003**	2.725	**0.020**
Crystalline Fe(III)	6.532	**0.001**	1.729	0.185	0.449	0.843
Non-sulfidic Fe(II)	69.071	< **0.001**	0.176	0.839	1.920	0.090
FeS	57.327	< **0.001**	2.684	0.075	2.228	0.050
FeS_2	60.469	< **0.001**	2.146	0.125	0.536	0.779
Fe(III):Fe(II) ratios	178.109	< **0.001**	5.637	**0.005**	0.980	0.446
Rates						
Dissimilatory FeR	37.464	< **0.001**	4.066	**0.021**	1.018	0.421
Sulfide-mediated FeR	13.660	< **0.001**	3.095	0.052	2.079	0.067

Bold letter denotes the significant difference $p < 0.05$

Table 3 Soil and porewater geochemistry, and Fe(III) reduction (FeR) rates (integrating three tidal marsh plant species) among the rhizosphere, inner bulk soil (0–5 mm), middle bulk soil (5–15 mm), and outer bulk soil (15–100 mm) at the study site in the Min River estuary of the East China Sea in July 2016. All data were given in mean ± standard error ($n = 3$)

	Rhizobox			
	Rhizosphere	Inner bulk soil (0–5 mm)	Middle bulk soil (5–15 mm)	Outer bulk soil (15–100 mm)
Porewater geochemistry				
DOC (mg C L^{-1}) *	60.4 ± 1.6 ^{a}	36.2 ± 1.1 ^{b}	16.5 ± 1.1 ^{c}	15.2 ± 0.8 ^{c}
DON (mg N L^{-1}) *	3.6 ± 0.1 ^{a}	2.4 ± 0.1 ^{b}	1.3 ± 0.1 ^{c}	1.3 ± 0.1 ^{c}
SO_4^{2-} (mM) *	6.5 ± 0.2 ^{a}	6.0 ± 0.1 ^{a}	4.6 ± 0.1 ^{b}	3.8 ± 0.1 ^{c}
Fe^{2+} (μM) *	682 ± 20 ^{a}	461 ± 14 ^{b}	186 ± 14 ^{c}	159 ± 10 ^{c}
Soil geochemistry				
Poorly crystalline Fe(III) (μmol Fe g^{-1}) *	95.2 ± 3.5 ^{a}	68.7 ± 2.5 ^{b}	46.9 ± 2.5 ^{c}	34.2 ± 1.7 ^{d}
Crystalline Fe(III) (μmol Fe g^{-1}) *	64.0 ± 2.5 ^{a}	57.3 ± 1.7 ^{ab}	54.5 ± 1.7 ^{b}	52.6 ± 1.2 ^{b}
Non-sulfidic Fe(II) (μmol Fe g^{-1}) *	21.8 ± 2.3 ^{d}	29.3 ± 1.7 ^{c}	42.2 ± 1.7 ^{b}	52.1 ± 1.2 ^{a}
FeS (μmol Fe g^{-1}) *	1.5 ± 1.5 ^{c}	5.2 ± 1.0 ^{c}	10.2 ± 1.0 ^{b}	18.2 ± 0.7 ^{a}
FeS_2 (μmol Fe g^{-1}) *	9.3 ± 0.9 ^{d}	12.6 ± 0.7 ^{c}	16.0 ± 0.7 ^{b}	20.8 ± 0.5 ^{a}
Fe(III):Fe(II) ratios *	5.1 ± 0.2 ^{a}	2.8 ± 0.1 ^{b}	1.5 ± 0.1 ^{c}	0.9 ± 0.1 ^{d}
Rates (μmol Fe g^{-1} d^{-1})				
Dissimilatory FeR *	42.5 ± 2.7 ^{a}	38.9 ± 1.9 ^{ab}	34.0 ± 1.9 ^{b}	19.1 ± 1.3 ^{c}
Sulfide-mediated FeR *	1.7 ± 0.1 ^{a}	1.5 ± 0.1 ^{a}	1.1 ± 0.1 ^{b}	1.0 ± 0.1 ^{b}

*The parameters were significantly different among the rhizobox zones according to *Tukey* test at $p < 0.05$, levels are indicated by different letters

(9.1–9.6%) and *Bacillus* (4.8–5.6%) were the most abundant iron reducers (Table 5). Total iron reducers accounted for 14.6–15.7% of the total bacteria in the rhizosphere and declined to 1.4–2.1% in the bulk soil (Table 5).

Discussion

Iron speciation and mineralogy surrounding the root zone

The presence of marsh plant roots is considered to significantly influence Fe speciation in macro habitats (Gribsholt and Kristensen 2002; Kostka et al. 2002). Less attention is received on the radial distribution of Fe speciation in the root zone. In the current study, both poorly crystalline and crystalline Fe(III) concentrations were found enriched in the rhizosphere (Table 3 and Fig. 4). The larger Fe(III) pool is precipitated here because of radial oxygen loss (Khan et al. 2016). In addition, higher DOC concentrations in the rhizosphere (Fig. 3a) could also help stabilize a portion of Fe(III) complex (Jones et al. 2011; Li et al. 2015; Otero et al. 2006). The concentrations of the major reduced Fe species (i.e., non-sulfidic Fe(II) and Fe sulfides) were found at a relatively low level in the rhizosphere (Fig. 4). The rapid oxidation of Fe(II) closing the roots actually facilitates the diffusion of Fe(II) from the bulk soil to the rhizosphere (Yang et al. 2012). As a special case, porewater Fe^{2+} levels were relatively higher in the rhizosphere than in the bulk soil (Fig. 3d). A similar result was also reported by Sundby et al. (2003), who suggested porewater Fe^{2+} and dissolved O_2 were both detected in the root zone. There were two possible and not exclusive reasons for this: i) Fe(III) mineral could adsorb Fe^{2+} newly yielded by FeR to the mineral surfaces (Weston et al. 2006); ii) Fe sulfide was oxidized in the root zone and produced porewater SO_4^{2-} and Fe^{2+} (Ferreira et al. 2007). The second explanation also corresponded with the higher concentrations of SO_4^{2-} in the rhizosphere than bulk soil (Fig. 3c). Away from the root surface, decreasing Fe(III):Fe(II) ratios indicated a more reducing and anaerobic environment compared to the rhizosphere (Fig. 4). The concentrations of poorly crystalline and crystalline Fe(III) apparently declined in the bulk

Table 4 Soil and porewater geochemistry and Fe(III) reduction (FeR) rates (integrating four rhizobox zones) among *Phragmites australis*, *Spartina alterniflora*, and *Cyperus malaccensis* rhizoboxes, at the study site in the Min River estuary of the East China Sea, in July 2016. All data were given in mean ± standard error (n = 3)

	Tidal marsh plants		
	P. australis	*S.alterniflora*	*C. malaccensis*
Porewater geochemistry			
DOC (mg C L^{-1}) *	19.0 ± 8.6 ^{c}	32.0 ± 9.8 ^{a}	24.6 ± 9.2 ^{b}
DON (mg N L^{-1}) *	1.4 ± 0.4 ^{c}	2.2 ± 0.6 ^{a}	1.8 ± 0.6 ^{b}
SO_4^{2-} (mM) †	4.6 ± 0.6 ^{a}	5.1 ± 0.6 ^{a}	4.5 ± 0.9 ^{a}
Fe^{2+} (μM) †	284 ± 121 ^{a}	313 ± 137 ^{a}	275 ± 93 ^{a}
Soil geochemistry			
Poorly crystalline Fe(III) (μmol Fe g^{-1}) *	52.6 ± 16.2 ^{a}	57.6 ± 10.1 ^{a}	44.3 ± 13.7 ^{b}
Crystalline Fe(III) (μmol Fe g^{-1}) †	57.7 ± 4.9 ^{a}	52.8 ± 3.6 ^{a}	55.5 ± 5.0 ^{a}
Non-sulfidic Fe(II) (μmol Fe g^{-1}) †	39.7 ± 6.8 ^{a}	41.6 ± 7.3 ^{a}	43.1 ± 9.1 ^{a}
FeS (μmol Fe g^{-1}) †	10.3 ± 4.5 ^{a}	11.9 ± 5.3 ^{a}	12.9 ± 3.8 ^{a}
FeS_2 (μmol Fe g^{-1}) †	16.4 ± 3.0 ^{a}	15.9 ± 2.9 ^{a}	17.5 ± 2.8 ^{a}
Fe(III):Fe(II) ratios *	2.0 ± 0.8 ^{ab}	2.1 ± 0.9 ^{a}	1.7 ± 0.7 ^{b}
Rates (μmol Fe g^{-1} d^{-1})			
Dissimilatory FeR *	29.5 ± 6.6 ^{ab}	32.3 ± 8.7 ^{a}	26.5 ± 6.3 ^{b}
Sulfide-mediated FeR †	1.2 ± 0.2 ^{a}	1.3 ± 0.3 ^{a}	1.2 ± 0.2 ^{a}

*The parameters were significantly different among the plants according to *Tukey* test at $p < 0.05$, levels are indicated by different letters; † denoted the parameters were insignificantly different among the plants; $p > 0.05$

soil (Fig. 4). Besides, the poorly crystalline Fe(III) concentrations decreased more sharply compared to crystalline Fe(III) (Fig. 4), indicating that rhizosphere processes had a greater effect on poorly crystalline Fe(III). Non-sulfidic Fe(II) and Fe sulfides became the dominant Fe species in the bulk soil (Fig. 4). The change of dominant iron species from rhizosphere to bulk soil indicated a certain iron geochemical zonation pattern mediated by rhizosphere processes.

Approximately 60% of the rhizosphere Fe(III) was poorly crystalline, and this proportion declined to about 39% in the outer bulk soil. This finding coincided with results reported by Weiss et al. (2004, 2005), who suggested that the poorly crystalline Fe(III) accounted for 66 ± 7% of total Fe(III) in the rhizosphere, and 23 ± 7% of that in the bulk soil of *Typha latifolia* (a common freshwater emergent macrophyte). Poorly crystalline Fe(III) was also identified via SEM (Seyfferth 2015;

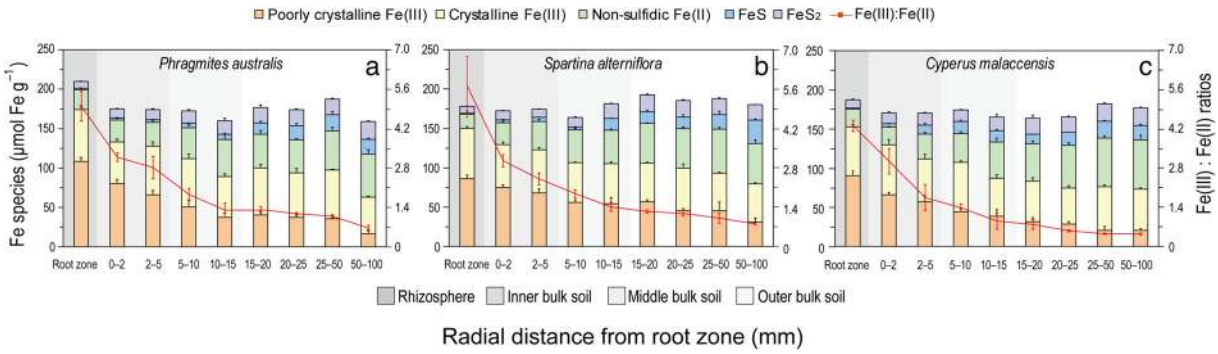

Fig. 4 Accumulation bar charts of solid-phase Fe species (poorly crystalline Fe(III), crystalline Fe(III), non-sulfidic Fe(II), FeS, and FeS_2) and Fe(III):Fe(II) ratios ($n = 3$; error bars indicate ± SE), in the soil of rhizoboxes of three marsh plants of the Min River estuary of the East China Sea in 2016 containing (a) *Phragmites australis*, (b) *Spartina alterniflora*, and (c) *Cyperus malaccensis*

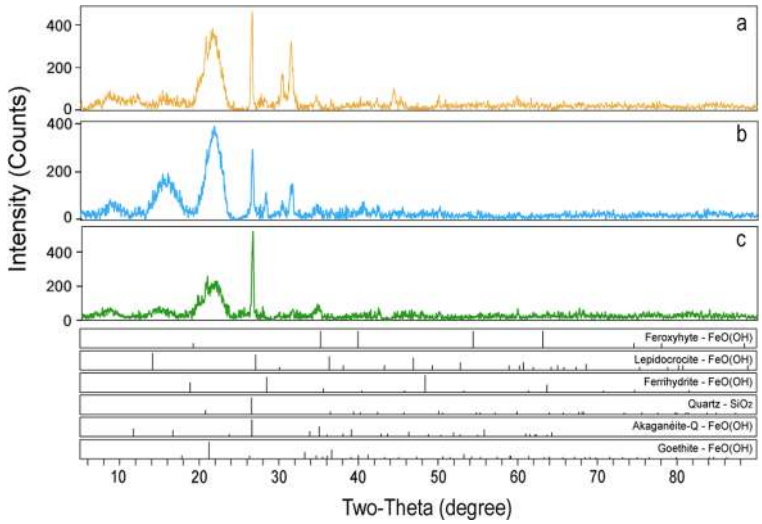

Fig. 5 X-ray diffraction diagrams of rhizosphere Fe(III) minerals and Quartz in the rhizoboxes of three marsh plants in the Min River estuary in the East China Sea in 2016: (**a**) *Phragmites australis*, (**b**) *Spartina alterniflora*, and (**c**) *Cyperus malaccensis*

Taggart et al. 2009), X-ray absorption near-edge structure spectroscopy (XANES) (Lin et al. 2010), and K-edge X-ray absorption fine structure spectroscopy (EXAFS) (Liu et al. 2006). According to our XRD results, poorly crystalline Fe(III), primarily in the form of feroxyhite, ferrihydrite, and lepidocrocite minerals was identified in the rhizosphere (Fig. 5). Poorly crystalline Fe(III) was newly deposited and mainly precipitated as a result of Fe(II) reoxidation (Seyfferth et al. 2011). In light of the presence of crystallization inhibitors like organic acids around the roots, only a very small amount of poorly crystalline Fe(III) could be transformed into the crystalline state (Cornell and Schwertmann 2003). Therefore, rhizosphere processes favored the precipitation of poorly crystalline Fe(III) over crystalline Fe(III). Compared to crystalline Fe(III), poorly crystalline Fe(III) was shown to have a larger specific surface area and higher thermodynamic properties and was considered to be more bioavailable and chemically active (Hyacinthe et al. 2006; Li et al. 2012). Combined, Fe(III) minerals were not only more abundant but also more bioavailable than those in the bulk soil.

Iron reducers between rhizosphere and bulk soil

Marsh plant roots typically have large populations of microbes, especially iron reducers (King and Garey 1999; Weiss et al. 2003). In our rhizoboxes, iron reducers were found to be a significant component of the total rhizosphere microbial community (Table 5). This was also found in a survey of freshwater marshes and saltmarshes in Virginia and Maryland (USA), where iron reducers (acetate-utilized type), accounted for an average of 7% of all bacterial cells in the rhizosphere of marsh plants, while in the bulk soil they accounted for < 1% of the total bacteria (Weiss et al. 2003). Iron reducers found in the root zone also contained both facultative and obligate anaerobe species in the current study. This result indicated the heterogeneity of the aerobic zone in the rhizosphere. We hypothesized that iron reducers could colonize on the micro-scale anaerobic zone of the root surface, such as the cytoderm of root epidermal cells (Neubauer et al. 2008), which have a 10–20 μm width according to previous micrography (Armstrong et al. 1991; Khan et al. 2016). This narrow area would also be an available ecological niche for iron reducers.

The abundance of the fermentative iron reducers *Clostridium* were found to be much less than *Geobacter* but higher than the *Anaeromyxobacter* and *Shewanella* (Table 5). Compared to dissimilatory iron reducers in tidal marsh ecosystems (Neubauer et al. 2005), little attention has been paid to the role of fermentative iron reducers. Nevertheless, *Clostridium* and *Bacillus* have been demonstrated as abundant and widespread in anaerobic Fe-rich paddy soil (Jia et al. 2015; Jia et al. 2018; Li et al. 2011; Zhuang et al. 2015). Fermentative Fe(III) reducers could use Fe(III) as electron sinks with intermediate metabolites, e.g., low-molecular-weight organic acids and hydrogen (Jia et al. 2018; Lentini et al. 2012). This finding suggested that fermentative Fe(III) reducers play a supporting and important role in the iron reducers community.

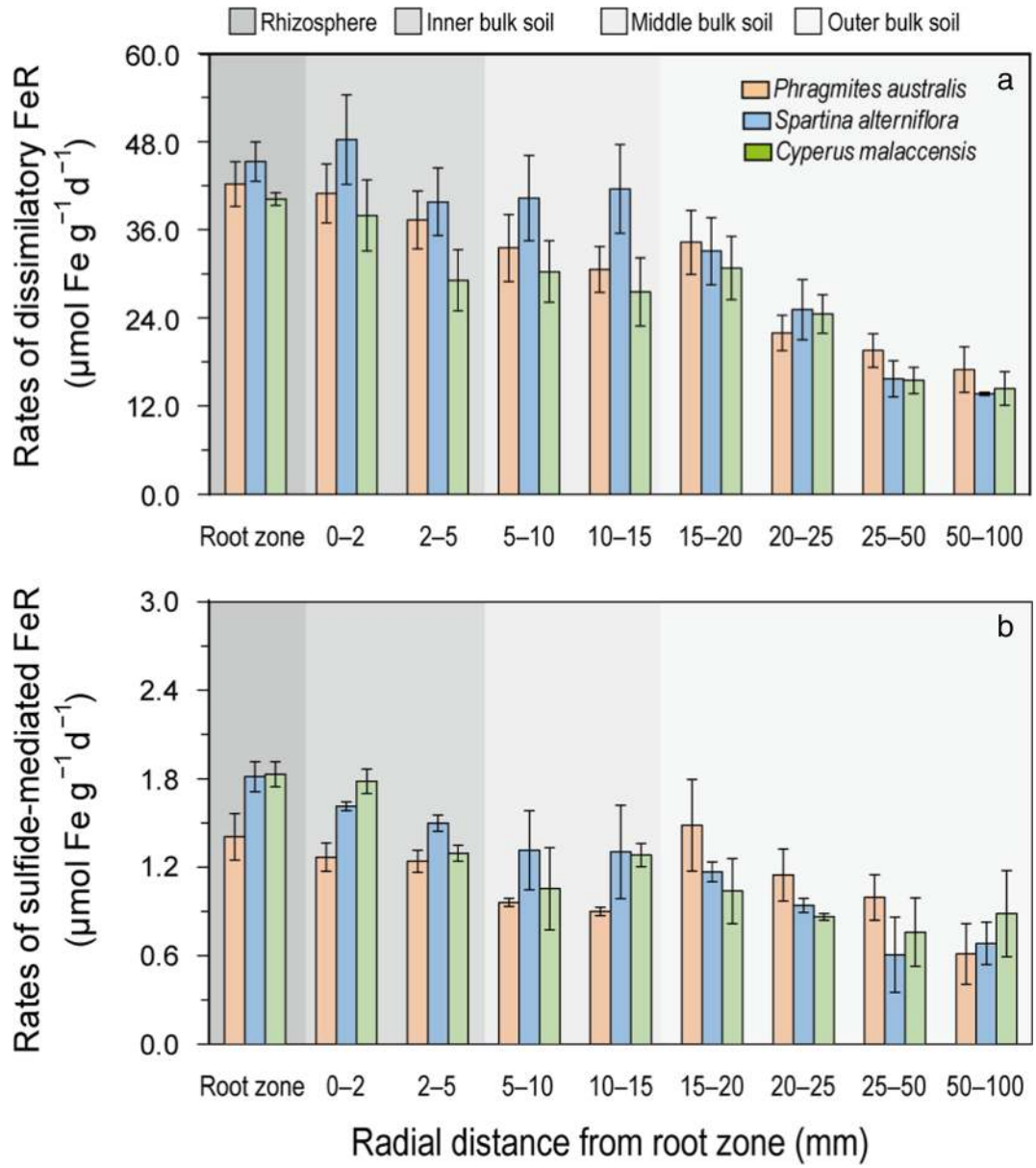

Fig. 6 Radial profiles (n = 3; error bars indicate ± SE) of dissimilatory Fe(III) reduction (FeR, given in μmol Fe g^{-1} d^{-1}) (**a**), and sulfide-mediated FeR (given in μmol Fe g^{-1} d^{-1}) (**b**), in the soil of rhizoboxes in the Min River estuary in the East China Sea in 2016: *Phragmites australis*, *Spartina alterniflora*, and *Cyperus malaccensis*

Effect of rhizosphere processes on dissimilatory Fe(III) reduction

The rates of dissimilatory FeR were significantly correlated with the concentrations of poorly crystalline Fe(III), DOC, and Fe(III):Fe(II) ratios (Fig. 7). The allocation of the poorly crystalline Fe(III) and Fe(III):Fe(II) ratios was strongly associated with root Fe plaque precipitation and radial oxygen loss, respectively (Armstrong et al. 2000; Khan et al. 2016), while the DOC concentrations were mainly derived from root exudation (el Zahar Haichar et al. 2014). Herein, rhizosphere processes deeply affected the rates of dissimilatory FeR around the roots. The rates of dissimilatory FeR of the three marsh plants generally decreased in a logarithmic form, away from the rhizosphere into bulk soil (Fig. 8). Different decay patterns of dissimilatory FeR rates were observed among three tidal marsh plants (Fig. 8). The soil in the

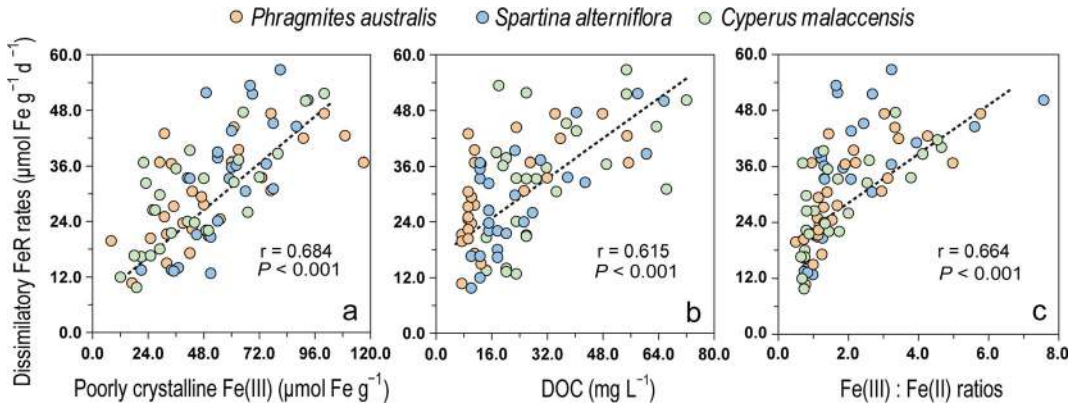

Fig. 7 Correlations between rates of dissimilatory Fe(III) reduction (FeR) and: (**a**) poorly crystalline Fe(III), (**b**) DOC, and (**c**) Fe(III):Fe(II) ratios ($n = 81$), in rhizoboxes in the Min River estuary in the East China Sea in 2016: *Phragmites australis*, *Spartina alterniflora*, and *Cyperus malaccensis*

C. malaccensis rhizoboxes had a sharper decreasing gradient and maintained a relatively lower value in the outer bulk soil than in the *P. australis* and *S. alterniflora* rhizoboxes (Fig. 8). Given that the belowground biomass was comparable among the three tidal marsh plants in the rhizoboxes (Table 1), interspecies differences of dissimilatory FeR among three marsh plants could be explained by their root porosity and aerenchyma (Table 1). Root porosity and aerenchyma are both one of the important guarantees for root oxygen releasing (Armstrong et al. 2000). Root porosity and SEM photos in this study suggested that *S. alterniflora* and *P. australis* grew a more-developed aerenchyma (i.e., larger air space) than *C. malaccensis* (Table 1 and Fig. 2). Likewise, a previous study conducted adjacent to our study site, also revealed that the root of *C. malaccensis* were composed of densely packed cells in the exodermis with a small percentage of air space, compared with *P. australis* and *S. alterniflora* (Tong et al. 2012). Moreover, root porosity had a close relationship with the concentrations of rhizosphere poorly crystalline Fe(III), and Fe(III):Fe(II) ratios (see supplementary materials Fig. S2). All these results suggested

Table 5 Total bacteria and iron reducers (±SE; n = 3) among *Phragmites australis*, *Spartina alterniflora*, and *Cyperus malaccensis* rhizoboxes, at the study site in the Min River estuary of the East China Sea in July 2016

Bacteria (10^7 copies g^{-1})		Tidal marsh plants		
		P. australis	*S.alterniflora*	*C. malaccensis*
Geobacter	Rhizosphere	1758 ± 118 (9.1%)	1581 ± 102 (9.6%)	1324 ± 43 (9.1%)
	Bulk soil	158 ± 14 (1.3%)	216 ± 25 (1.6%)	157 ± 22 (1.1%)
Bacillus	Rhizosphere	938 ± 86 (4.8%)	921 ± 34 (5.6%)	702 ± 11 (4.8%)
	Bulk soil	1 ± 0 (0.0%)	13 ± 1 (0.1%)	70 ± 8 (0.5%)
Shewanella	Rhizosphere	65 ± 2 (0.3%)	32 ± 1 (0.2%)	29 ± 4 (0.4%)
	Bulk soil	15 ± 1 (0.1%)	20 ± 2 (0.2%)	24 ± 2 (0.2%)
Clostridium	Rhizosphere	35 ± 6 (0.2%)	24 ± 2 (0.1%)	89 ± 12 (1.2%)
	Bulk soil	1 ± 0 (0.0%)	5 ± 1 (0.1%)	28 ± 1 (0.3%)
Anaeromyxobacter	Rhizosphere	19 ± 10 (0.1%)	15 ± 8 (0.1%)	9 ± 2 (0.1%)
	Bulk soil	3 ± 0 (0.0%)	9 ± 3 (0.1%)	10 ± 2 (0.1%)
∑Fe(III) reducers	Rhizosphere	2816 ± 113 (14.6%)	2580 ± 107 (15.7%)	2279 ± 58 (15.7%)
	Bulk soil	179 ± 15 (1.4%)	329 ± 8 (2.0%)	356 ± 38 (2.1%)
Total bacteria	Rhizosphere	19,389 ± 1121	16,442 ± 146	14,565 ± 564
	Bulk soil	12,648 ± 690	13,496 ± 182	13,982 ± 673

that root porosity and aerenchyma contribute to the interspecies difference of dissimilatory FeR in the root zone of tidal marsh plants.

Though *S. alterniflora* and *P. australis* had similar root porosity, as well as a poorly crystalline Fe(III) pool, and Fe(III):Fe(II) ratios (Table 4), there was still a minor difference of dissimilatory FeR rates between the two plants (Fig. 8). In accordance with this, *S. alterniflora* had a larger DOC and DON pool compared to *P. australis* and *C. malaccensis* (Table 4). This may be determined as due to *S. alterniflora* being an invasive plant in the Min River estuary (Tong et al. 2012). The invasive species *S. alterniflora,* is always found to transfer more C to bulk soil compared to native species (Bradford et al. 2012; Zhang et al. 2017). Thus, different DOC and DON pools in the rhizoboxes could at least partially explain the interspecies difference of dissimilatory FeR, between *S. alterniflora* and *P. australis*.

Implication for rhizosphere carbon cycling

Dissimilatory FeR was much stronger compared to the sulfide-mediated FeR (Fig. 6) and dominated the majority of the total FeR in the tidal marsh soil. Similar results were reported in the tidal marshes of the Han River estuary, Korea, where dissimilatory FeR accounted for greater than 90% of the total FeR (Hyun et al. 2009; Hyun et al. 2007). These results suggested that the presence of roots increased the importance of microbial Fe(III) respiration in the rhizosphere. Dissimilatory FeR has been associated with the organic carbon mineralization (Eq. 2), while sulfide-mediated FeR was connected with dissimilatory SR (Eqs. 3 and 4). The dissimilatory FeR and SR could be estimated by Eqs. 2 to 4 and presented in C units using the theoretical stoichiometry of C:Fe = 1:4 and S:C = 2:1 (Kostka et al. 2002; Kristensen et al. 2011; Hyun et al. 2009):

$$4FeOOH + CH_3COO^- + 8H^+ = CO_2 + 7H_2O + 4Fe^{2+} \quad (2)$$

$$SO_4^{2-} + CH_3COO^- + 3H^+ = 2CO_2 + 2H_2O + H_2S \quad (3)$$

$$2FeOOH + 3H_2S = 2FeS + S_0 + 4H_2O \quad (4)$$

In this perspective, rates of dissimilatory FeR were 10.6 and 4.8 μmol C g^{-1} d^{-1} in the rhizosphere and outer bulk soil, respectively; while rates of dissimilatory SR were 5.1 and 3.0 μmol C g^{-1} d^{-1} in the rhizosphere and the outer bulk soil, respectively. According to this result, dissimilatory FeR outcompeted dissimilatory SR in both the rhizosphere and outer bulk soil, but the relative importance of FeR gradually declined away from the root surface. Therefore, rhizosphere processes may also induce a shift of the dominant pathway of organic carbon mineralization from rhizosphere to bulk soil, and furthermore reshape corresponding microbial community structure in the root zone.

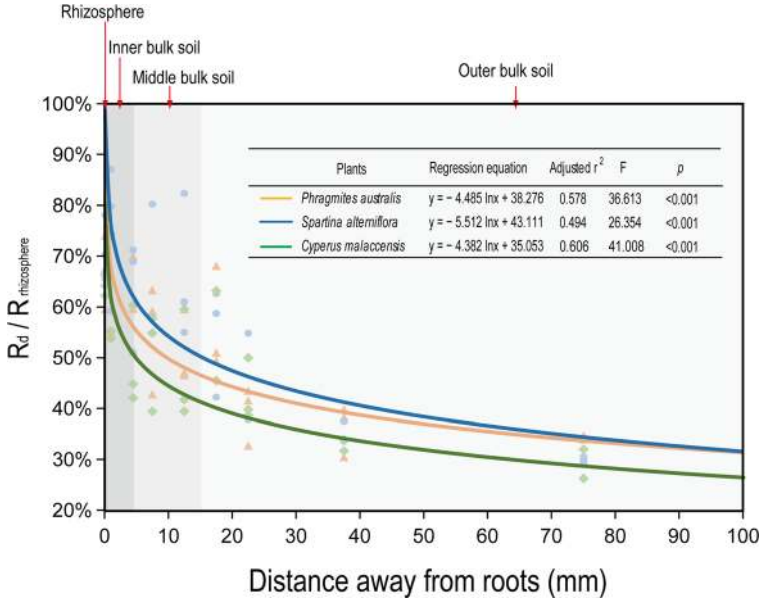

Fig. 8 The change of R_d normalized $R_{rhizosphere}$ along the radial distance away from the rhizosphere in rhizoboxes in the Min River estuary in the East China Sea in 2016: *Phragmites australis*, *Spartina alterniflora*, and *Cyperus malaccensis*. R_d denoted as the rates of dissimilatory FeR at certain distance away from roots; $R_{rhizosphere}$ denoted as the rates of dissimilatory FeR in the rhizosphere

Conclusions

Though the rhizosphere is typically characterized as a zone of Fe(III) deposition, our results suggested that the presence of tidal marsh plant roots also favored rapid dissimilatory FeR in the tidal marsh soils. For the first time, a radial, millimeter-scale shift of the Fe speciation, rates of dissimilatory FeR, and population of iron reducers was reported between the rhizosphere and bulk soil. Rhizosphere processes and plant species both mediated changes in the dissimilatory FeR in the tidal marsh system. The radial change of dissimilatory FeR rates was affected by the allocation of poorly crystalline Fe(III) and dissolved organic carbon in the root zone. The interspecies difference of dissimilatory FeR, was affected by the root porosity and root aerenchyma of tidal marsh plants. For the future work, intensive studies on the shift of the dominant organic carbon mineralization pathway in the root zone are needed.

Acknowledgments This work was financially supported by the National Science Foundation of China (Grant No. 41501252), the Science Foundation of Fujian Province (Grant No. 2016 J05097), Key Laboratory of wet Subtropical Ecology and geography process of Ministry of Education (Grant No. 2017KFJJ02), Key Laboratory of Coastal Environmental Processes and Ecological Remediation, YICCAS (Grant No. 2018KFJJ10), and the Open Test Fund for valuable instruments and equipment from Fuzhou University (2018 T013). We thank the Elsevier Web shop for its assistance with language editing during the preparation of this manuscript.

References

APHA (2005) American public health association. In: Eaton AD, Franson MAH (eds) Standard methods for the examination of water and wastewater, 21st edn. American Public Health Association, Washington, pp 3576–3578

Armstrong W, Justin SHFW, Beckett PM, Lythe S (1991) Root adaptation to soil waterlogging. Aquat Bot 39:57–73

Armstrong W, Cousins D, Armstrong J, Turner D, Beckett P (2000) Oxygen distribution in wetland plant roots and permeability barriers to gas-exchange with the rhizosphere: a microelectrode and modelling study with *Phragmites australis*. Ann Bot 86:687–703

Beck M, Dellwig O, Holstein JM, Grunwald M, Liebezeit G, Schnetger B, Brumsack H-J (2008) Sulphate, dissolved organic carbon, nutrients and terminal metabolic products in deep pore waters of an intertidal flat. Biogeochemistry 89: 221–238

Bell C, Carrillo Y, Boot CM, Rocca JD, Pendall E, Wallenstein MD (2014) Rhizosphere stoichiometry: are C:N:P ratios of plants, soils, and enzymes conserved at the plant species-level? New Phytol 201:505–517

Bradford MA, Strickland MS, DeVore JL, Maerz JC (2012) Root carbon flow from an invasive plant to belowground foodwebs. Plant Soil 359:233–244

Burton ED, Sullivan LA, Bush RT, Johnston SG, Keene AF (2008) A simple and inexpensive chromium-reducible sulfur method for acid-sulfate soils. Appl Geochem 23:2759–2766

Cline JD (1969) Spectrophotometric determination of hydrogen sulfide in natural waters. Limnol Oceanogr 14:454–458

Colmer TD, Pedersen O (2008) Oxygen dynamics in submerged rice (*Oryza sativa*). New Phytol 178:326–334

Colombo C, Palumbo G, He J-Z, Pinton R, Cesco S (2014) Review on iron availability in soil: interaction of Fe minerals, plants, and microbes. J Soils Sediments 14:538–548

Cornell RM, Schwertmann U (2003) The iron oxides: structure, properties, reactions, occurrence and uses. Wiley-VCH Press. Weinheim, Germany, pp 2–3

Crowder AA, Macfie SM (1986) Seasonal deposition of ferric hydroxide plaque on roots of wetland plants. Can J Bot 64: 2120–2124

el Zahar Haichar F, Santaella C, Heulin T, Achouak W (2014) Root exudates mediated interactions belowground. Soil Biol Biochem 77:69–80

Emerson D, Fleming EJ, Mcbeth JM (2010) Iron-oxidizing bacteria: an environmental and genomic perspective. Annu Rev Microbiol 64:561–583

Ferreira T, Otero X, Vidal-Torrado P, Macías F (2007) Effects of bioturbation by root and crab activity on iron and sulfur biogeochemistry in mangrove substrate. Geoderma 142:36–46

Finzi AC, Abramoff RZ, Spiller KS, Brzostek ER, Darby BA, Kramer MA, Phillips RP (2015) Rhizosphere processes are quantitatively important components of terrestrial carbon and nutrient cycles. Glob Chang Biol 21:2082–2094

Gribsholt B, Kristensen E (2002) Effects of bioturbation and plant roots on salt marsh biogeochemistry: a mesocosm study. Mar Ecol-prog Ser 241:71–87

Hafner S, Wiesenberg GL, Stolnikova E, Merz K, Kuzyakov Y (2014) Spatial distribution and turnover of root-derived carbon in alfalfa rhizosphere depending on top-and subsoil properties and mycorrhization. Plant Soil 380:101–115

Hartmann A, Schmid M, Tuinen DV, Berg G (2009) Plant-driven selection of microbes. Plant Soil 321:235–257

Hines ME, Knollmeyer SL, Tugel JB (1989) Sulfate reduction and other sedimentary biogeochemistry in a northern New England salt marsh. Limnol Oceanogr 34:578–590

Hinsinger P, Bengough AG, Vetterlein D, Young IM (2009) Rhizosphere: biophysics, biogeochemistry and ecological relevance. Plant Soil 321:117–152

Holmes DE, Finneran KT, O'Neil RA, Lovley DR (2002) Enrichment of members of the family *Geobacteraceae* associated with stimulation of dissimilatory metal reduction in uranium-contaminated aquifer sediments. Appl Environ Microbiol 68:2300–2306

Howarth R (1993) Microbial processes in salt-marsh sediments. Aquat Microbiol:239–260

Howarth RW, Jørgensen BB (1984) Formation of ^{35}S-labelled elemental sulfur and pyrite in coastal marine sediments (Limfjorden and Kysing Fjord, Denmark) during short-term

$^{35}SO_4^{2-}$ reduction measurements. Geochim Cosmochim Ac 48:1807–1818

Hung CH, Cheng CH, Cheng LH, Liang CM, Lin CY (2008) Application of *Clostridium*-specific PCR primers on the analysis of dark fermentation hydrogen-producing bacterial community. Int J Hydrogen Energ 33:1586–1592

Hyacinthe C, Bonneville S, Van Cappellen P (2006) Reactive iron(III) in sediments: chemical versus microbial extractions. Geochim Cosmochim Ac 70: 4166–4180

Hyun J-H, Smith AC, Kostka JE (2007) Relative contributions of sulfate-and iron(III) reduction to organic matter mineralization and process controls in contrasting habitats of the Georgia saltmarsh. Appl Geochem 22:2637–2651

Hyun J-H, Mok J-S, Cho H-Y, Kim S-H, Lee KS, Kostka JE (2009) Rapid organic matter mineralization coupled to iron cycling in intertidal mud flats of the Han River estuary, Yellow Sea. Biogeochemistry 92:231–245

Jia R, Li L-N, Qu D (2015) pH shift-mediated dehydrogenation and hydrogen production are responsible for microbial iron (III) reduction in submerged paddy soils. J Soils Sediments 15:1178–1190

Jia R, Li L, Qu D, Mi N (2018) Enhanced iron (III) reduction following amendment of paddy soils with biochar and glucose modified biochar. Environ Sci Pollut R 25:91–103

Johnston SG, Keene AF, Bush RT, Burton ED, Sullivan LA, Isaacson L, McElnea AE, Ahern CR, Smith CD, Powell B (2011) Iron geochemical zonation in a tidally inundated acid sulfate soil wetland. Chem Geol 280:257–270

Jones ME, Beckler JS, Taillefert M (2011) The flux of soluble organic-iron(III) complexes from sediments represents a source of stable iron(III) to estuarine waters and to the continental shelf. Limnol Oceanogr 56:1811–1823

Karanfil T, Erdogan I, Schlautman MA (2003) Selecting filter membranes for measuring DOC and UV_{254}. J Am Water Works Assoc 95:86–100

Khan N, Seshadri B, Bolan N, Saint CP, Kirkham MB, Chowdhury S, Yamaguchi N, Lee DY, Li G, Kunhikrishnan A (2016) Root iron plaque on wetland plants as a dynamic pool of nutrients and contaminants. Adv Agron 138:1–96

King G, Garey MA (1999) Ferric iron reduction by bacteria associated with the roots of freshwater and marine macrophytes. Appl Environ Microbiol 65:4393–4398

Kirwan ML, Mudd SM (2012) Response of salt-marsh carbon accumulation to climate change. Nature 489:550–553

Kludze HK, DeLaune RD, Patrick WH (1993) Aerenchyma formation and methane and oxygen exchange in rice. Soil Sci Soc Am J 57:386–391

Koop-Jakobsen K, Wenzhöfer F (2015) The dynamics of plant-mediated sediment oxygenation in *Spartina anglica* rhizospheres-a planar optode study. Estuar Coasts 38:951–963

Koop-Jakobsen K, Fischer J, Wenzhöfer F (2017) Survey of sediment oxygenation in rhizospheres of the saltmarsh grass-*Spartina anglica*. Sci Total Environ 589:191–199

Kostka JE, Luther GW III (1994) Partitioning and speciation of solid phase iron in saltmarsh sediments. Geochim Cosmochim Ac 58:1701–1710

Kostka JE, Roychoudhury A, Van Cappellen P (2002) Rates and controls of anaerobic microbial respiration across spatial and temporal gradients in saltmarsh sediments. Biogeochemistry 60: 49–76

Kristensen E, Mangion P, Tang M, Flindt MR, Holmer M, Ulomi S (2011) Microbial carbon oxidation rates and pathways in sediments of two Tanzanian mangrove forests. Biogeochemistry 103:143–158

Laanbroek H (1990) Bacterial cycling of minerals that affect plant growth in waterlogged soils: a review. Aquat Bot 38:109–125

Lambers H, Mougel C, Jaillard B, Hinsinger P (2009) Plant-microbe-soil interactions in the rhizosphere: an evolutionary perspective. Plant Soil 321:83–115

Lemanceau P, Bauer P, Kraemer S, Briat JF (2009) Iron dynamics in the rhizosphere as a case study for analyzing interactions between soils, plants and microbes. Plant Soil 321:513–535

Lentini CJ, Wankel SD, Hansel CM (2012) Enriched iron (III)-reducing bacterial communities are shaped by carbon substrate and iron oxide mineralogy. Front Microbiol 3:404

Li YL, Fan XR, Shen QR (2008) The relationship between rhizosphere nitrification and nitrogen-use efficiency in rice plants. Plant Cell Environ 31:73–85

Li H, Peng J, Weber KA, Zhu Y (2011) Phylogenetic diversity of Fe (III)-reducing microorganisms in rice paddy soil: enrichment cultures with different short-chain fatty acids as electron donors. J Soils Sediments 11:1234–1242

Li X, Liu T, Li F, Zhang W, Zhou S, Li Y (2012) Reduction of structural Fe(III) in oxyhydroxides by *Shewanella decolorationis* S12 and characterization of the surface properties of iron minerals. J Soils Sediments 12:217–227

Li H, Huang G, Meng Q, Ma L, Yuan L, Wang F, Zhang W, Cui Z, Shen J, Chen X (2013) Integrated soil and plant phosphorus management for crop and environment in China. A review Plant soil 349:157–167

Li X, Hou L, Liu M, Zheng Y, Yin G, Lin X, Cheng L, Li Y, Hu X (2015) Evidence of nitrogen loss from anaerobic ammonium oxidation coupled with ferric iron reduction in an intertidal wetland. Environ Sci Technol 49:11560–11568

Lin H, Shi J, Bei W, Yang J, Chen Y, Zhao Y, Hu T (2010) Speciation and biochemical transformations of sulfur and copper in rice rhizosphere and bulk soil-XANES evidence of sulfur and copper associations. J Soils Sediments 10:907–914

Liu W, Zhu Y, Hu Y, Williams P, Gault A, Meharg A, Charnock J, Smith F (2006) Arsenic sequestration in Iron plaque, its accumulation and speciation in mature Rice plants (*Oryza Sativa L.*). Environ Sci Technol 40:5730–5736

Longstreth DJ, Borkhsenious ON (2000) Root cell ultrastructure in developing aerenchyma tissue of three wetland species. Ann Bot 86:641–646

Lovley DR, Phillips EJ (1986) Organic matter mineralization with reduction of ferric iron in anaerobic sediments. Appl Environ Microbiol 51:683–689

Luo M, Zeng C-S, Tong C, Huang J-F, Yu Q, Guo Y-B, Wang S-H (2014) Abundance and speciation of iron across a subtropical tidal marsh of the Min River estuary in the East China Sea. Appl Geochem 45:1–13

Luo M, Huang J, Tong C, Liu Y, Duan X, Hu Y (2017) Iron dynamics in a subtropical estuarine tidal marsh: the roles of seasonality and plants. Mar Ecol-prog Ser 577:1–15

Ma X-M, Zarebanadkouki M, Kuzyakov Y, Blagodatskaya E, Pausch J, Razavi BS (2018) Spatial patterns of enzyme activities in the rhizosphere: effects of root hairs and root radius. Soil Biol Biochem 118:69–78

Mitsch WJ, Gosselink JG (2015) Tidal marshes. In wetlands, 5th edn. John Wiley & Sons, Inc, Hoboken, pp 259–310

Moeslundi L, Thamdrup B, Jørgensen BB (1994) Sulfur and iron cycling in a coastal sediment: radiotracer studies and seasonal dynamics. Biogeochemistry 27:129–152

Muyzer G, Teske A, Wirsen CO, Jannasch HW (1995) Phylogenetic relationships of *Thiomicrospira* species and their identification in deep-sea hydrothermal vent samples by denaturing gradient gel electrophoresis of 16S rDNA fragments. Arch Microbiol 164:165–172

Neubauer SC, Givler K, Valentine SK, Megonigal JP (2005) Seasonal patterns and plant-mediated controls of subsurface wetland biogeochemistry. Ecology 86:3334–3344

Neubauer SC, Toledo-Durán GE, Emerson D, Megonigal JP (2007) Returning to their roots: Iron-oxidizing Bacteria enhance short-term plaque formation in the wetland-plant rhizosphere. Geomicrobiol J 24:65–73

Neubauer S, Emerson D, Megonigal J (2008) Microbial oxidation and reduction of iron in the root zone and influences on metal mobility. John Wiley and Sons, Hoboken, NJ, pp 339–371

Otero X, Ferreira T, Vidal-Torrado P, Macías F (2006) Spatial variation in pore water geochemistry in a mangrove system (Pai Matos island, Cananeia-Brazil). Appl Geochem 21: 2171–2186

Peng Q-A, Shaaban M, Wu Y, Hu R, Wang B, Wang J (2016) The diversity of iron reducing bacteria communities in subtropical paddy soils of China. Appl Soil Ecol 101:20–27

Poulton SW, Canfield DE (2005) Development of a sequential extraction procedure for iron: implications for iron partitioning in continentally derived particulates. Chem Geol 214:209–221

Roden EE, Wetzel RG (2002) Kinetics of microbial Fe(III) oxide reduction in freshwater wetland sediments. Limnol Oceanogr 47:198–211

Schulze D (1981) Identification of soil iron oxide minerals by differential X-ray diffraction. Soil Sci Soc Am J 45:437–440

Seeberg-Elverfeldt J, Schlüter M, Feseker T, Kölling M (2005) Rhizon sampling of pore waters near the sediment/water interface of aquatic systems. Limnol Oceanogr Methods 3: 361–371

Seyfferth AL (2015) Abiotic effects of dissolved oxyanions on iron plaque quantity and mineral composition in a simulated rhizosphere. Plant Soil 397:43–61

Seyfferth AL, Webb SM, Andrews JC, Fendorf S (2011) Defining the distribution of arsenic species and plant nutrients in rice (*Oryza sativa L.*) from the root to the grain. Geochim Cosmochim Ac 75:6655–6671

Snoeyenbos-West OL, Nevin KP, Anderson RT, Lovley DR (2000) Enrichment of *Geobacter* species in response to stimulation of Fe(III) reduction in sandy aquifer sediments. Microb Ecol 39:153–167

St-Cyr L, Crowder AA (1989) Factors affecting iron plaque on the roots of *Phragmites australis (Cav.) Trin. ex Steudel*. Plant Soil 116:85–93

Sundby B, Vale C, Caetano M, Luther Iii GW (2003) Redox chemistry in the root zone of a salt marsh sediment in the Tagus estuary, Portugal. Aquat Geochem 9:257–271

Taggart MA, Mateo R, Charnock JM, Bahrami F, Green AJ, Meharg AA (2009) Arsenic rich iron plaque on macrophyte roots-an ecotoxicological risk? Environ Pollut 157:946–954

Tong C, Wang W-Q, Huang J-F, Gauci V, Zhang L-H, Zeng C-S (2012) Invasive alien plants increase CH_4 emissions from a subtropical tidal estuarine wetland. Biogeochemistry 111: 677–693

Wang J, Vollrath S, Behrends T, Bodelier PLE, Muyzer G, Meimafranke M, Oudsten FD, Cappellen PV, Laanbroek HJ (2011) Distribution and diversity of *Gallionella*-like neutrophilic iron oxidizers in a tidal freshwater marsh. Appl Environ Microbiol 77:2337–2344

Wang X, Chen R, Jing Z, Yao T, Feng Y, Lin X (2018) Root derived carbon transport extends the rhizosphere of rice compared to wheat. Soil Biol Biochem 122:211–219

Weber KA, Achenbach LA, Coates JD (2006) Microorganisms pumping iron: anaerobic microbial iron oxidation and reduction. Nat Rev Microbiol 4:752–764

Weiss JV, Emerson D, Backer SM, Megonigal JP (2003) Enumeration of Fe(II)-oxidizing and Fe(III)-reducing bacteria in the root zone of wetland plants: implications for a rhizosphere iron cycle. Biogeochemistry 64:77–96

Weiss JV, Emerson D, Megonigal JP (2004) Geochemical control of microbial Fe(III) reduction potential in wetlands: comparison of the rhizosphere to non-rhizosphere soil. FEMS Microbiol Ecol 48:89–100

Weiss JV, Emerson D, Megonigal JP (2005) Rhizosphere Iron(III) deposition and reduction in a *L.*-dominated wetland. Soil Sci Soc Am J 69:1861–1870

Weiss JV, Rentz JA, Plaia T, Neubauer SC, Merrill-Floyd M, Lilburn T, Bradburne C, Megonigal JP, Emerson D (2007) Characterization of neutrophilic Fe(II)-oxidizing Bacteria isolated from the rhizosphere of wetland plants and description of *Ferritrophicum radicicola gen. nov. sp. nov.*, and *Sideroxydans paludicola sp. nov.* Geomicrobiol J 24:559–570

Weston NB, Dixon RE, Joye SB (2006) Ramifications of increased salinity in tidal freshwater sediments: geochemistry and microbial pathways of organic matter mineralization. J Geophys Res-Biogeo 111(2005–2012):1–14

Whitmire S, Hamilton S (2008) Rates of anaerobic microbial metabolism in wetlands of divergent hydrology on a glacial landscape. Wetlands 28:703–714

Wu Q, Sanford RA, Löffler FE (2006a) Uranium(VI) reduction by *Anaeromyxobacter dehalogenans* strain 2CP-C. Appl Environ Microbiol 72:3608–3614

Wu S, Zhong J, Huan L (2006b) Genetics of subpeptin JM4-a and subpeptin JM4-B production by *Bacillus* subtilis JM4. Biochem Bioph Res Co 344:1147–1154

Yang JX, Liu Y, Zhi-Hong YE (2012) Root-induced changes of pH, eh, Fe(II) and fractions of Pb and Zn in rhizosphere soils of four wetland plants with different radial oxygen losses. Pedosphere 22:518–527

Yang J, Tam NF-Y, Ye Z (2014) Root porosity, radial oxygen loss and iron plaque on roots of wetland plants in relation to zinc tolerance and accumulation. Plant Soil 374:815–828

Zhang P, Nie M, Li B, Wu J (2017) The transfer and allocation of newly fixed C by invasive *Spartina alterniflora* and native *Phragmites australis* to soil microbiota. Soil Biol Biochem 113:231–239

Zhuang L, Xu J, Tang J, Zhou S (2015) Effect of ferrihydrite biomineralization on methanogenesis in an anaerobic incubation from paddy soil. J Geophys Res-Biogeo 120:876–886